Research on Protection of Tuning Area Equipment Disconnection in the ZPW-2000A Track Circuit*

Yunshui Zheng[1], *Zhanyi Shu*[1*] *and Shenglin Gao*[2]

(1. College of Automation & Electrical Engineering, Lanzhou Jiaotong University, Lanzhou 730070, China;
2. CRSC Research & Design Institute Group Co., Ltd., Beijing 100070, China)

Abstract: To overcome the problem of tuning area faults influencing the normal operation of the ZPW-2000A track circuit, protector models are established to protect the track circuit from interference. First, the parameters of the protector models are calculated according to the circuit resonance principle. Second, a four-terminal network model of the track circuit in a normal state is established according to transmission-line theory and the transmission equations are derived. Third, the rail voltage is simulated, and an experimental platform is built to verify the models. Finally, the transmission equations of the protectors are derived, and the variation of the rail voltage is analyzed. The results indicate that tuning area faults have significant influence on the rail voltage. However, the installation of protectors can effectively reduce the influence, and not bear on the normal operation and maintenance of the track circuit, which significantly improves the protection ability of the track circuit against tuning area faults.

Keywords: Tuning area faults, protector model, rail voltage, experimental platform, normal state

1 Introduction

The ZPW-2000A track circuit system is widely used in China. However, tuning area faults can lead to the transmission of over-zone signals in different sections and frequently cause potential trouble. At present, most of the studies on tuning areas focus on only fault diagnosis or simulation analysis of the track circuit.

In recent years, many studies on the interference signals of track circuits have been conducted by establishing models and simulations. Zhao et al. [1] studied the influence of interference from adjacent sections on locomotive signal equipment. A model of the track circuit in the locomotive signal state was established to analyze the interference, which is the over-zone signals from adjacent sections. Wang et al. [2] built models of tuning area faults in the locomotive signal state and analyzed the induced voltage of the locomotive signal. According to the variation of frequency characteristics of the track circuit components. Xu et al. [3] established frequency varying models of the track circuit and analyzed the interference from adjacent sections. Mariscotti et al. [4] established an audio track circuit model using transmission-line theory and analyzed the transmission characteristics of simulated S-type tuning units. The impedance of the track circuits was calculated and the variation of the rail voltage was analyzed. Additionally, the values of return current and harmonics of a track circuit in the shunting state were measured and analyzed. Beak et al.[5] presented measurement method at the interference of return current to the signal system. By comparing the test results with the standard, the safety of the system affected by the interference was evaluated. The interference signal of the arc from adjacent sections was measured and transmission equations of the arc were deduced [6]. Chen et al. [7] built a hardware simulation platform and analyzed track circuit transmission characteristics through the platform, which is useful for diagnosing track circuit faults. The above studies that focused on interference have made great contributions to establishing protection scheme models and verifying the protection

Manuscript received November 21, 2019; revised March 30, 2020; accepted July 1, 2020. Date of publication March 31, 2021; date of current version August 24, 2020.

* Corresponding Author, E-mail: 525402925@qq.com

* Supported by the National Natural Science Foundation of China (61763023).
Digital Object Identifier: 10.23919/CJEE.2021.000010

ability of the protectors.

Numerous researches have also focused on track circuit protection. Yu et al. [8] proposed a treatment method using insulated steel bars in the tuning area to prevent interference in a jointless track circuit. The interference was decreased by improving the isolation ability of the conductors in the tuning area, but maintenance was difficult to implement with track circuit faults because the conductors were embedded in a ballastless board. Won et al. [9] analyzed the voltage variations of the transmitter and receiver, and a resonance circuit was designed using a compensation capacitor installed on the rail to reduce impedance. This research verified that installing protectors on the railroad could improve the transmission characteristics, but protectors were only used to balance the resistance of the railroad. Nomura et al. [10] designed a resonance capacitor and connected it with the impedance bond of the track circuit. Its safety was verified in the lightning strike position. This research is beneficial for analyzing the safety of protectors, but it was not applied to preventing the over-zone signal. Wu et al.[11-12] studied the damaged insulation of the track circuit in the ZPW-2000A station and designed a choke adaptation transformer to protect the receivers, obtaining good results through test and verification. They designed a protection scheme to protect the over-zone signal in the station by installing a resonance circuit in the choke transformer, which was also applied to the rail in the tuning area. Ma et al. [13] researched and verified a protection method to diminish resonance interference, but it was applied to only the vehicles. There are also many resonance circuits applied to electrical systems, which can ensure safety and improve transmission ability [14-16].

Most of these researchers considered maintainability [17], but research efforts were less focused on fault protection abilities. Therefore, qualitative and quantitative analysis of track circuit protection ability against tuning area faults is necessary to design, operate, maintain and formulate train control systems. A second-stage zero-impedance device is set to further prevent the over-zone signal to improve fault protection ability if necessary [18].

In this study, protector parameters are calculated and models of track circuits with protectors have been built. The protection ability of the track circuit against tuning area faults is verified by simulation.

2 Working principle and protection scheme

2.1 Working principle of the track circuit

The ZPW-2000A track circuit can be divided into five parts: transmission channel, transmitter tuning area, main track circuit, receiver tuning area, and receiving channel [19]. The adjacent sections are electrically isolated using the resonance circuit of the tuning area. The above protection scheme refers to the redundancy method. The first compensation capacitor beside the tuning area is replaced by a zero-impedance device to isolate the interference signal from the adjacent track sections. The specific location is shown in Fig. 1. When the equipment works normally, the

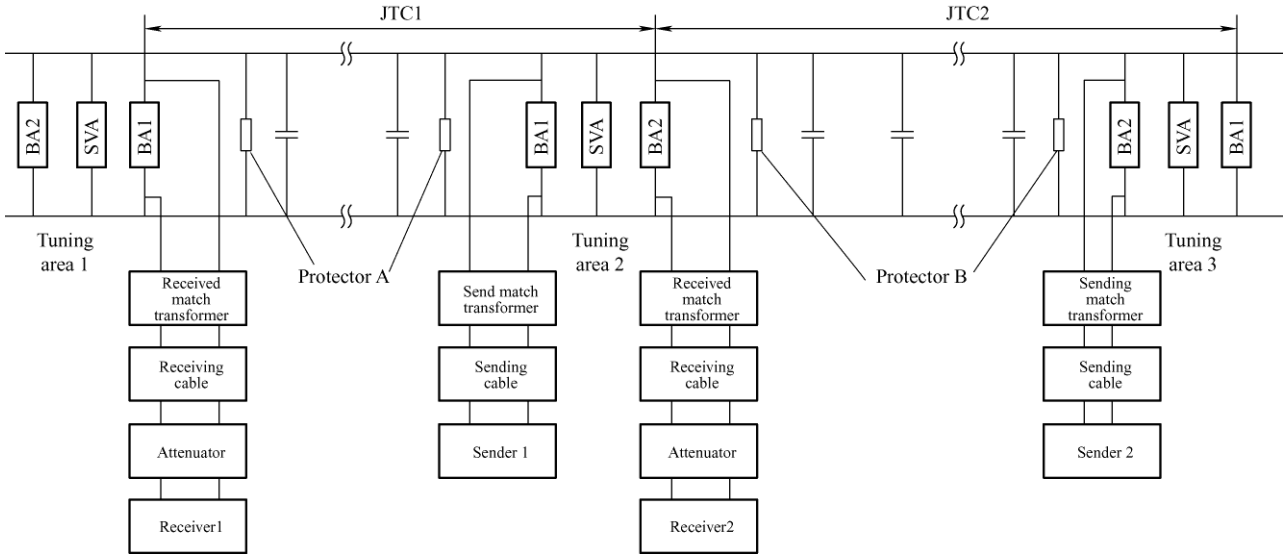

Fig. 1 Structure of the ZPW-2000A track circuit

protection device is equivalent to a compensation capacitor for its own section. When the tuning unit fails, the protector can be equivalent to a zero-impedance device. The basic structure of the ZPW-2000A track circuit with protectors is shown in Fig. 1, and the structure of the tuning area is shown in Fig. 2. JTC1 represents jointless track circuit 1 and JTC2 represents jointless track circuit 2.

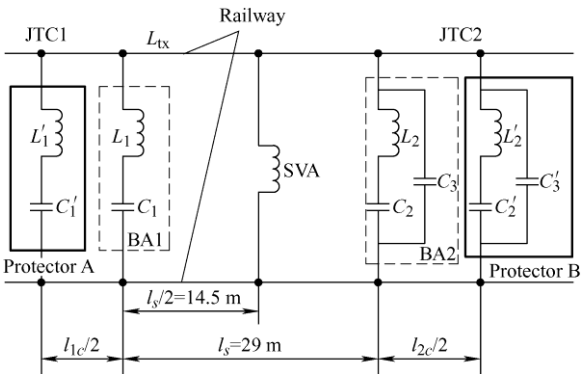

Fig. 2 Tuning area (little track circuit)

The equipment in the tuning area includes tuning unit BA1, hollow coil SVA, and tuning unit BA2. The step length of the equipment is $l_s/2$, and the impedance of each rail section is L_{tx}. When the equipment in the tuning area fails, the impedance value becomes lower, resulting in over-zone signal transmission. To improve the fault protection ability, it is necessary to install protectors on the rail. Because of the fixed position of the rail drilling, the position of the protectors is at the first compensation capacitor near the tuning area. The structure of protector A and protector B is the same as that of the tuning units, but their parameters are different. The structure is shown in Fig. 2.

2.2 Protection scheme

According to Figs. 2 and 3, tuning unit BA1 is composed of an inductive element, L_1, and a capacitive element, C_1, in series. For signal f_2 of the adjacent JTC2, a series resonance is formed, and the interference signal of the adjacent section is short-circuited. Tuning unit BA2 is composed of an inductive element, L_2, a capacitor element, C_2, in series, and a capacitor element, C_3, in parallel. L_2 and C_2 form a series resonance for the signal f_1 of JTC1. As shown in Fig. 3a, BA1 is capacitive to f_1, and BA2 is short-circuited to f_1. BA1 and hollow coil SVA, as well as four rails with step lengths of $l_s/2$, form a parallel resonance to present extreme impedance to f_1. In case of a BA2 open-circuit fault, protector B has a series resonance to f_1, which

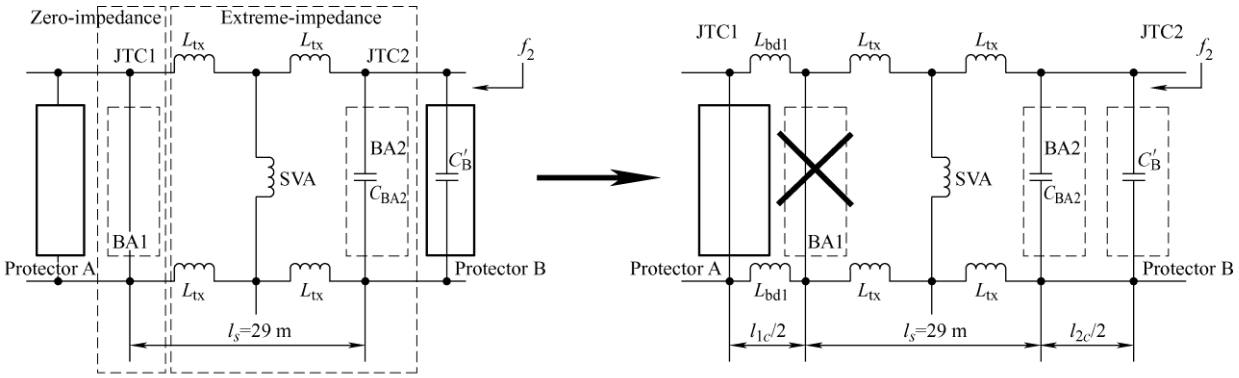

(a) Working principle of protector A

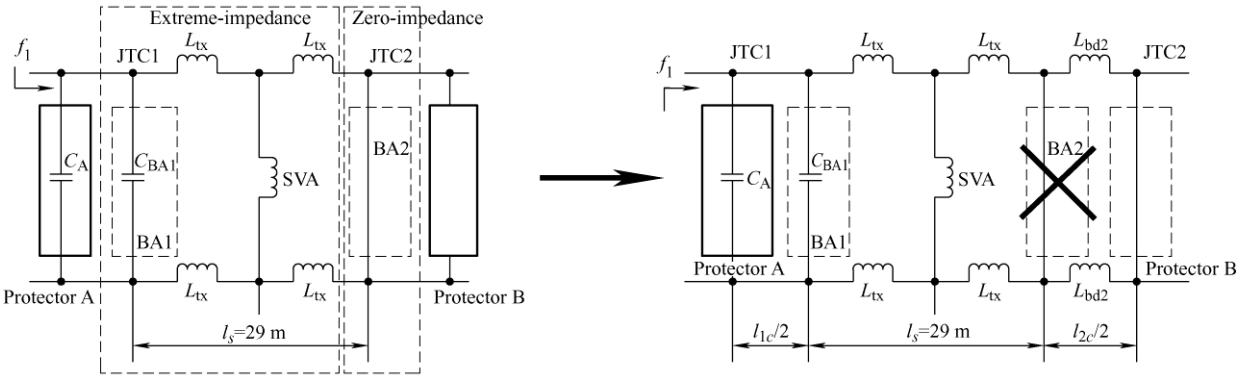

(b) Working principle of protector B

Fig. 3 Working principle of the protection scheme

protects f_1 from over-zone transmission. Similarly, as shown in Fig. 3b, L_2 and C_2 of BA2 form a series resonance to f_1. BA2 is capacitive to f_2 and forms a parallel resonance with SVA and four rails. When BA1 fails, protector A has a series resonance with f_2, which protects f_2 from over-zone transmission. There is no effect on the track voltage with the short-circuit equipment, so only the protection of broken equipment is considered.

2.3 Parameter calculation

According to circuit principles, the formulas for calculating the impedance parameters of tuning area elements are given by

$$Z_{\mathrm{BA1}} = j\omega L_1 + \frac{1}{j\omega C_1} \qquad Z_{\mathrm{SVA}} = j\omega L_{\mathrm{SVA}}$$

$$Z_{\mathrm{BA2}} = \left(\left(j\omega L_2 + \frac{1}{j\omega C_2}\right)\cdot\frac{1}{j\omega C_3}\right)\Big/\left(\left(j\omega L_2 + \frac{1}{j\omega C_2}\right) + \frac{1}{j\omega C_3}\right) \tag{1}$$

where Z_{BA1} represents the impedance of BA1, Z_{BA2} represents the impedance of BA2, and Z_{SVA} represents the impedance of SVA.

Because of the different frequencies of track sections, the angular frequency of JTC1 is ω_1, that of JTC2 is ω_2, and $\omega_2 > \omega_1$. According to Eq. (1) and the circuit resonance principle, the two elements of protector A satisfy the following relationship

$$\omega_2 = \frac{1}{\sqrt{L_1' C_1'}} \tag{2}$$

Because $\omega_2 > \omega_1$, the relationship between L_1' and C_1' is derived as

$$C_1' < \frac{1}{\omega_1^2 L_1'} \tag{3}$$

Because the capacitance value of protector A is the same as that of the compensation capacitor, its impedance, Z_{cA}, can be described as

$$Z_{cA} = j\omega L_1' + \frac{1}{j\omega C_1'} = \frac{1-\omega^2 L_1' C_1'}{j\omega C_1'} = 1\Big/\left(j\omega\frac{C_1'}{1-\omega^2 L_1' C_1'}\right) \tag{4}$$

It can be seen from Eq. (4) that if protector A is capacitive to this section, its capacitance value can be derived as

$$C_{\mathrm{A}} = \frac{C_1'}{1-\omega_1^2 L_1' C_1'} \tag{5}$$

At this time, C_{A} is connected in parallel with the hollow coil SVA and some rails. This ensures that protector A is capacitive to this section and that capacitor C_{A} is equal to the original compensation capacitor.

Similarly, L_2' and C_2' of protector B have a series resonance to f_1, satisfying the following relationship

$$\omega_1 = \frac{1}{\sqrt{L_2' C_2'}} \tag{6}$$

Because $\omega_2 > \omega_1$, the relationship between L_2' and C_2' is as follows

$$L_2' > \frac{1}{\omega_2^2 C_2'} \tag{7}$$

$$L_{\mathrm{B}} = L_2' - \frac{1}{\omega_2^2 C_2'} \tag{8}$$

Because the capacitance of protector B is equal to that of the compensation capacitor, its impedance Z_{cB} can be derived as

$$Z_{cB} = \left(j\omega L_{\mathrm{B}}\cdot\frac{1}{j\omega C_3'}\right)\Big/\left(j\omega L_{\mathrm{B}} + \frac{1}{j\omega C_3'}\right) = 1\Big/\left(j\omega\frac{\omega^2 L_{\mathrm{B}} C_3' - 1}{\omega^2 L_{\mathrm{B}}}\right) \tag{9}$$

where L_{B} represents the inductance value of L_2 and C_2 in series, and L_{B} and C_3' are connected in parallel. After calculation, the equivalent capacitor value is C_{B}, and its parameters need to meet the requirements. C_{B} can be described as

$$C_{\mathrm{B}} = C_3' - \frac{1}{\omega_2^2 L_{\mathrm{B}}} \tag{10}$$

C_{B} needs to be connected in parallel with SVA to ensure that the capacitor value of protector B is equal to that of the compensation capacitor.

3 Model of the over-zone frequency

In this study, a hierarchical modeling method is used to establish a four-terminal network model of the track circuit in its normal state. According to the sampling points on the track, the main track is divided into a left half $\boldsymbol{T}_{\mathrm{L}}$, and a right half $\boldsymbol{T}_{\mathrm{R}}$, and then the transmission equations are derived.

The over-zone transmission model of the track circuit in its normal state is shown in Fig. 4. U_{s2}, $\boldsymbol{N}_{\mathrm{cb}}$, $\boldsymbol{N}_{\mathrm{sm}}$, $\boldsymbol{N}_{\mathrm{gnet}}$, $\boldsymbol{N}_{\mathrm{sxf}}$, and $\boldsymbol{N}_{\mathrm{rxf}}$ represent the equations of the transmitter voltage, transmission cable, matching

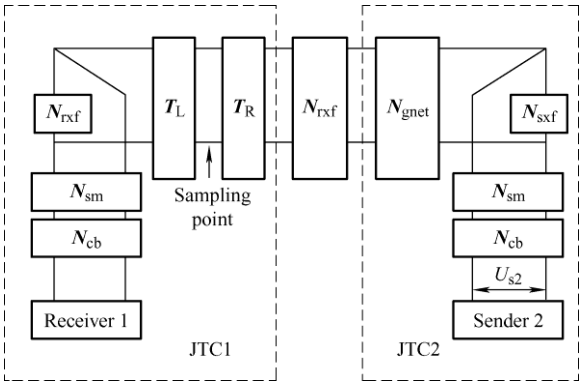

Fig. 4 Over-zone transmission model

transformer, JTC2 main track, sender, and receiver tuning area, respectively. Z_{s1} represents the apparent impedance of BA1 and Z_{j1} represents that of BA2. According to the structure of the main track circuit, $\boldsymbol{N}_{gnet}$ can be expressed as

$$\boldsymbol{N}_{gnet} = (\boldsymbol{T}_{cc})^n = (\boldsymbol{Tx}(l_c/2) \times \boldsymbol{T}_c \times \boldsymbol{Tx}(l_c/2))^n \tag{11}$$

where $\boldsymbol{T}_{cc}$ represents the transmission equation of the compensation capacitor unit model, $\boldsymbol{T}_c$ represents the transmission equation of the compensation capacitor, $\boldsymbol{Tx}(l_c/2)$ represents the rail transmission equation with a length of one half step of the compensation capacitor, and n is the number of compensation capacitors of JTC2. $\boldsymbol{N}_{sxf}$ contains three pieces of equipment: SVA, BA1, and BA2. Its transmission equation can be derived as

$$\boldsymbol{N}_{sxf} = \boldsymbol{T}_{sBA1} \times \begin{bmatrix} 1 & Z_{ca} \\ 0 & 1 \end{bmatrix} \times \begin{bmatrix} 1 & 0 \\ \dfrac{1}{Z_{tx}} & 1 \end{bmatrix} \tag{12}$$

where Z_{ca} represents the impedance of cables that connect the rail and tuning units and Z_{tx} is described as

$$\begin{aligned} \boldsymbol{T}_{SVA} &= \begin{bmatrix} 1 & 0 \\ \dfrac{1}{Z_{SVA}+Z_{ca}} & 1 \end{bmatrix} \\ \boldsymbol{T}_{tx} &= \boldsymbol{Tx}(l_s/2) \times \boldsymbol{T}_{SVA} \times \boldsymbol{Tx}(l_s/2) \\ Z_{tx} &= \frac{\boldsymbol{T}_{tx}(1,1)(Z_{BA2}+Z_{ca}) + \boldsymbol{T}_{tx}(1,2)}{\boldsymbol{T}_{tx}(2,1)(Z_{BA2}+Z_{ca}) + \boldsymbol{T}_{tx}(2,2)} \end{aligned} \tag{13}$$

Here, $\boldsymbol{T}_{SVA}$ represents the transmission equation of SVA, $\boldsymbol{T}_{tx}$ represents the transmission equation of an SVA unit, and Z_{tx} represents the impedance from BA1 of the sender in the adjacent track section to BA2 of the receiver in the track section. The structure of $\boldsymbol{N}_{rxf}$ is shown in Fig. 5.

In Fig. 5, Z_{gz1} represents the fault value of BA1, Z_{gz2} represents the fault value of BA2. $\boldsymbol{T}_{jBA2}$ represents

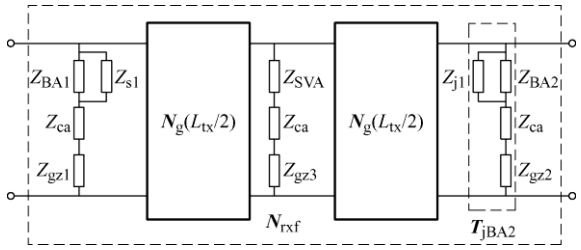

Fig. 5 Model of the tuning area

the transmission equation of BA2 at the receiver, which can be described as

$$\boldsymbol{T}_{jBA2} = \begin{bmatrix} 1 & 0 \\ \dfrac{1}{Z_{BA2}//Z_{j1}+Z_{ca}+Z_{gz2}} & 1 \end{bmatrix} \tag{14}$$

where Z_{j1} is expressed as

$$Z_{j1} = \frac{\boldsymbol{N}_{j11} \times Z_1 + \boldsymbol{N}_{j12}}{\boldsymbol{N}_{j21} \times Z_1 + \boldsymbol{N}_{j22}} \tag{15}$$

Here, Z_1 represents impedance value of the receiving end and analog cable network. Additionally, $\boldsymbol{N}_{j11}$, $\boldsymbol{N}_{j12}$, $\boldsymbol{N}_{j21}$, and $\boldsymbol{N}_{j22}$ are expressed by a four-terminal network, $\boldsymbol{N}_j$, which is equivalent to the transmission equation from the matching transformer at the receiving end to the transmission cable. This is expressed as

$$\boldsymbol{N}_j = \begin{bmatrix} \boldsymbol{N}_{j11} & \boldsymbol{N}_{j12} \\ \boldsymbol{N}_{j21} & \boldsymbol{N}_{j22} \end{bmatrix} = \boldsymbol{N}_{sm} \times \boldsymbol{N}_{cb} \tag{16}$$

where $\boldsymbol{N}_{cb}$ represents the transmission equation of cables and $\boldsymbol{N}_{sm}$ represents the transmission equation of matching transformer. The calculation of Z_{s1} is the same as that for Z_{j1}. The transmission $\boldsymbol{T}_{sBA1}$ of BA1 can be expressed as

$$\boldsymbol{T}_{sBA1} = \begin{bmatrix} 1 & 0 \\ \dfrac{1}{Z_{BA1}//Z_{s1}+Z_{ca}+Z_{gz1}} & 1 \end{bmatrix} \tag{17}$$

and the transmission of $\boldsymbol{N}_{rxf}$ can be described by

$$\boldsymbol{N}_{rxf} = \boldsymbol{T}_{jBA2} \times \boldsymbol{T}_{tx} \times \boldsymbol{T}_{sBA1} \tag{18}$$

Three position relationships between the sampling point and compensation capacitor in the main track are shown in Fig. 6.

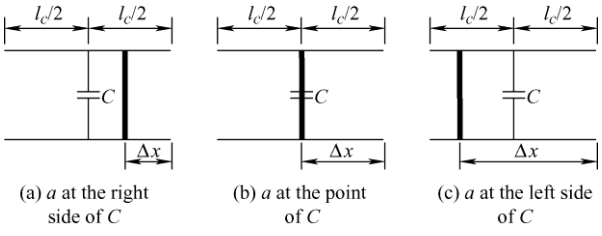

Fig. 6 Position of the sampling point

The distance from the sampling point to the right side of the m^{th} compensation capacitor module is Δx, and $\boldsymbol{T}_{\text{R}}$ is described by

$$\boldsymbol{T}_{\text{R}}(\Delta x)=\begin{cases}(\boldsymbol{T}_{\text{cc}})^{m}\times\boldsymbol{Tx}(\Delta x) & 0<\Delta x<l_c/2\\ (\boldsymbol{T}_{\text{cc}})^{m}\times\boldsymbol{Tx}(l_c/2)\times & \\ \boldsymbol{T}_{\text{c}}\times\boldsymbol{Tx}(\Delta x-l_c/2) & l_c/2<\Delta x<l_c\\ (\boldsymbol{T}_{\text{cc}})^{m} & \Delta x=0\\ (\boldsymbol{T}_{\text{cc}})^{m}\times\boldsymbol{Tx}(l_c/2) & \Delta x=l_c/2\end{cases} \tag{19}$$

The distance from the sampling point to the left side of the m^{th} compensation capacitor module is Δx_1, and $\boldsymbol{T}_{\text{L}}$ is described by

$$\boldsymbol{T}_{\text{L}}(\Delta x_1)=\begin{cases}\boldsymbol{Tx}(\Delta x_1-l_c/2)\times\boldsymbol{T}_{\text{c}}\times & \\ \boldsymbol{Tx}(l_c/2)\times(\boldsymbol{T}_{\text{cc}})^{n-1-m} & l_c/2<\Delta x_1<l_c\\ \boldsymbol{Tx}(\Delta x_1)\times(\boldsymbol{T}_{\text{cc}})^{n-1-m} & 0<\Delta x_1<l_c/2\\ (\boldsymbol{T}_{\text{cc}})^{n-m} & \Delta x_1=l_c\\ \boldsymbol{Tx}(l_c/2)\times(\boldsymbol{T}_{\text{cc}})^{n-1-m} & \Delta x_1=l_c/2\end{cases} \tag{20}$$

As Fig. 4 shows, if there is a fault in the tuning area, the values of Z_{gz1} and Z_{gz2} are used to simulate the open-circuit faults. The rail voltage is simulated, and the transmission equation from the sending end to the sampling point can be expressed as

$$\boldsymbol{NN}_1=\boldsymbol{N}_{\text{cb}}\times\boldsymbol{N}_{\text{sm}}\times\boldsymbol{N}_{\text{sxf}}\times\boldsymbol{N}_{\text{gnet}}\times\boldsymbol{N}_{\text{rxf}}\times\boldsymbol{T}_{\text{R}} \tag{21}$$

The transmission equation from the sampling point to the receiving end of the track circuit in this section is expressed as

$$\boldsymbol{NN}_2=\boldsymbol{T}_{\text{L}}\times\boldsymbol{N}_{\text{rxf}}\times\boldsymbol{N}_{\text{sm}}\times\boldsymbol{N}_{\text{cb}} \tag{22}$$

According to transmission-line theory, Z_z represents the transfer impedance of the sampling point, which is derived as

$$Z_z=\frac{\boldsymbol{NN}_2(1,1)\times Z_{\text{j}}+\boldsymbol{NN}_2(1,2)}{\boldsymbol{NN}_2(2,1)\times Z_{\text{j}}+\boldsymbol{NN}_2(2,2)} \tag{23}$$

The transmitter voltage is U_{s2}, and the sampling point voltage A_{f1} is described by

$$A_{f1}=\frac{U_{\text{s2}}}{\left|\boldsymbol{NN}_1(1,1)+\boldsymbol{NN}_1(1,2)/Z_z\right|} \tag{24}$$

4 Model verification and fault analysis

To calculate the rail voltage, it is necessary to determine the most unfavorable condition, which includes the lowest transmission voltage, highest rail impedance, and lowest ballast resistance.

4.1 Model validation

4.1.1 Laboratory platform construction

The experiments were conducted using the track circuit experimental platform shown in Fig. 7. ① to ③ represent sender 2, receiver 1, and sender 1 of the track circuit, respectively. ④ to ⑦ represent the attenuator, tuning area equipment, matching transformer, and transmission cable, respectively. ⑧ represents numerous compensation capacitors and ⑨ represents the main track simulator and sampling points with a step size of 25 m. Computers were used to place the sampling points and input the primary parameters. Fig. 7 shows the construction of the laboratory platform and Tab. 1 lists the main information of the platform equipment.

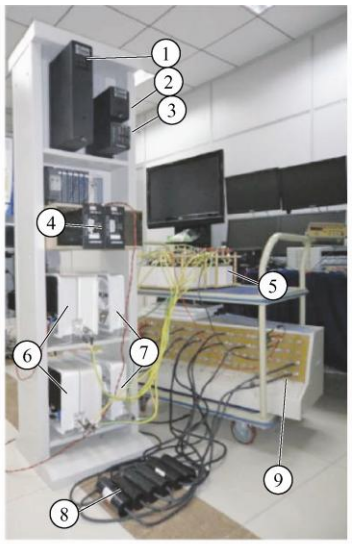

(a) Connection of main equipment on the platform

(b) Main track circuit

(c) Sampling point

Fig. 7 Construction of laboratory platform

According to the information in Fig. 7 and Tab. 1, a circuit connection diagram of the laboratory platform is shown in Fig. 8. The serial numbers correspond to the devices in the platform. Switches S_1 and S_2 represent the sending transmission channels of JTC1 and JTC2, respectively. These are used to distinguish signals from different track circuits in simulation and analyses.

Tab. 1 Equipment information

Number	Component		Information
①	Sender2		The voltage is 129.236 V, and the frequency is 1 700 Hz.
②	Receiver1		The impedance is 400 Ω, and the work voltage is 25 V.
③	Sender1		The voltage is 127.779 V, and the frequency is 2 300 Hz.
④	Attenuator		Improving transmission distance instead of transmission cable.
⑤	Matching transformer		It consists of two electrolytic capacitors with cables.
⑥	Tuning area equipment	BA1	The unit includes two components: L_1 = 37.145 μH and C_1 = 130.44 μF.
		BA2	The unit includes three components: L_2 = 93.472 μH, C_2 = 90.9 μF, and C_3 = 276.61 μF.
		SVA	L_{SVA} = 33.5 μH
⑦	Transmission cable		It consists of a number of cable units.
⑧	Compensation capacitor		55 μF, the number of compensation capacitors in JTC1 is 12.
⑨	Main track simulation panel		The length is 1 180 m, and the impedance is 15.1∠82.3° Ω • km
⑩	Computer		2.3 GHz, 500 GB, Windows 10; input the parameters and output simulation results.

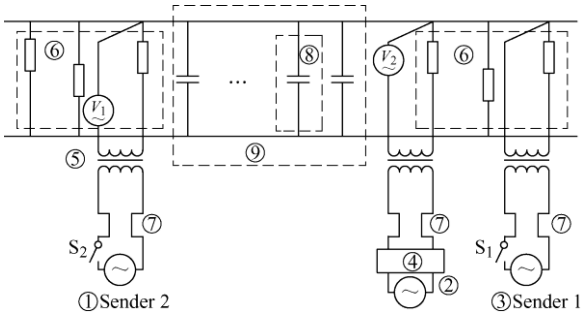

Fig. 8 Circuit connection diagram

According to Fig. 8, the method for measuring voltage is as follows.

(1) As shown in Figs. 7 and 8, the sampling point models of the main track panel with voltmeters have been connected in parallel. As shown in Fig. 7b, the compensation capacitors have been connected to the main track circuit by cables. The models of the sampling points are shown in Fig. 7c.

(2) When the switch S_1 is closed and the switch S_2 is open, the rail voltage of f_1 is measured by the voltmeters. Similarly, with switch S_2 closed and S_1 open, measure the rail voltages of f_2 by the voltmeters.

(3) The bolts which represent the sampling position on the main track panel have been connected with the models of the sampling points. With the voltmeters measure the voltage of the models of the sampling points, the rail voltages of sampling points have been obtained by the voltmeters.

4.1.2 Simulation of the rail voltage

According to Eqs. (12)-(24), the voltage simulation of track circuits is shown in Fig. 9.

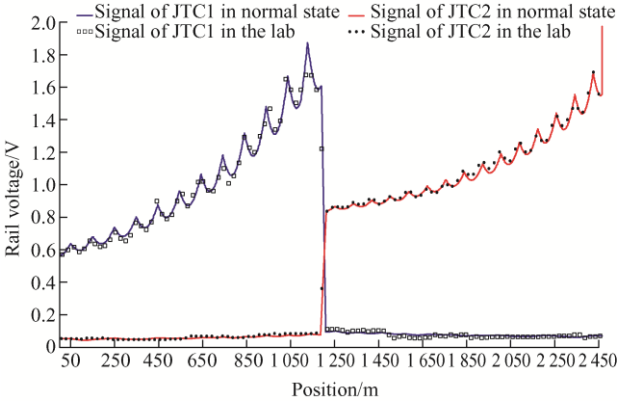

Fig. 9 Rail voltage in the normal state

It can be observed from Fig. 9 that the curves of rail voltage decline significantly after crossing the tuning area. Moreover, the curves of over-zone signals are like waves. The value of the rail voltage measured in the experiments is consistent with the simulation curve.

4.2 Simulation and analysis of tuning area faults

When the equipment is in an open-circuit condition, it can inevitably bear on the voltage in this section and adjacent sections. According to Fig. 1, the variation of impedance in the tuning area inevitably leads to an over-zone signal. As shown in Fig. 5, when BA1 fails, Z_{gz1} takes the value of ∞, 0.1, or 10. Similarly, Z_{gz2} and Z_{gz3} take the same value. With the tuning area faults, the impedance value changes. The curves are shown in Fig. 10.

According to Fig. 10a, with the open-circuit BA1, the extreme impedance decreases and the voltage

drops. The zero impedance has been destroyed and f_2 transmits to JTC1 across the area. According to Fig. 10b, the JTC1 zero impedance is destroyed and the voltage drops slightly. As the JTC2 extreme impedance

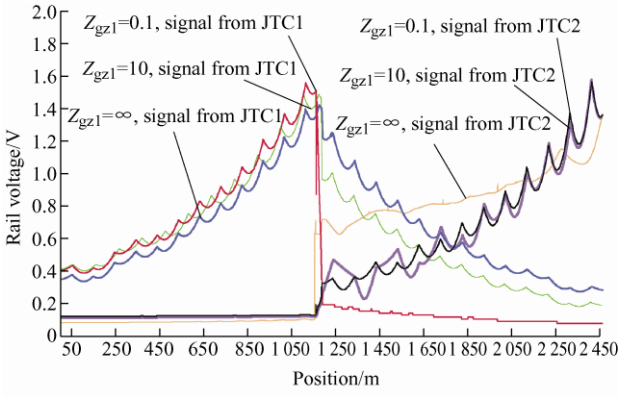

(a) Rail voltage of BA1 fault

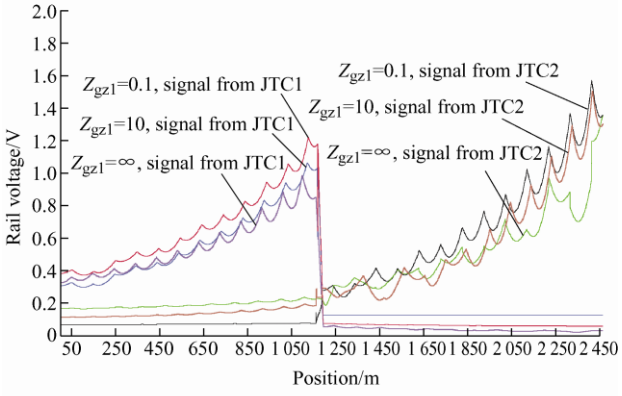

(b) Rail voltage of BA2 fault

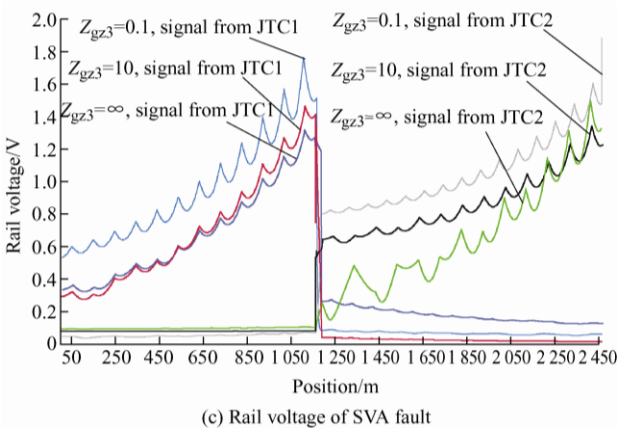

(c) Rail voltage of SVA fault

Fig. 10 Influence of different equipment faults in the tuning area

fails, the JTC1 voltage rises slightly. According to Fig. 10c, the rail voltage value has slightly decreased. This shows that the influence becomes considerably serious as the value of faults becomes larger, but the trends are similar. When the value is 0.1, the interference is too small to have an impact on the rail voltage. As a result, it is necessary to study the voltage when the value is ∞.

At this time, the variation of rail voltage affects both safety and efficiency. It is necessary to install protective devices to improve the track's protection ability against tuning area faults. The simulated results of the rail voltage of JTC without protectors are presented in Tab. 2.

Tab. 2 Rail voltage of tuning area faults of JTC without protectors

State of track circuit	Value of faults	f_1 signal in track section 1	f_2 signal in track section 1	f_1 signal in track section 2	f_2 signal in track section 2
Normal	0	2.931 5	0.026 3	0.051 8	0.533 1
BA1 fault	0.1	2.772 4	0.059 1	0.100 5	0.482 7
	10	1.845 9	0.184 6	0.232 1	0.309 4
	∞	1.539 0	0.233 7	0.267 2	0.257 5
BA2 fault	0.1	2.877 9	0.027 9	0.542 8	0.497 5
	10	2.694 7	0.398 6	1.995 6	0.382 4
	∞	2.615 8	0.043 1	2.213 4	0.331 2
SVA fault	0.1	2.915 4	0.039 4	0.147 1	0.502 6
	10	2.865 3	0.125 7	0.489 5	0.437 0
	∞	2.794 2	0.133 1	0.526 3	0.404 3

5 Verification of the protector model

To verify the correctness of the protector models, the simulation reflects the variation of the rail voltage. The transmission equations for the protector units (compared with the compensation capacitor unit) are given as

$$\boldsymbol{T}_{\mathrm{A}}=\begin{cases}\boldsymbol{Tx}(l_c/2)\times\begin{bmatrix}1 & 0\\ 1/Z_{cA} & 1\end{bmatrix}\times\boldsymbol{Tx}(l_c/2) & \text{Protector A}\\ \boldsymbol{Tx}(l_c/2)\times\begin{bmatrix}1 & 0\\ 1/Z_{cB} & 1\end{bmatrix}\times\boldsymbol{Tx}(l_c/2) & \text{Protector B}\end{cases} \tag{25}$$

The transmission equations for the main track circuit are as follows

$$\boldsymbol{T}_{\mathrm{R}}=\begin{cases}\boldsymbol{T}_{\mathrm{A}}\times(\boldsymbol{T}_{\mathrm{cc}})^{m-1}\times\boldsymbol{Tx}(\Delta x) & 0<\Delta x<l_c/2\\ \boldsymbol{T}_{\mathrm{A}}\times(\boldsymbol{T}_{\mathrm{cc}})^{m-1}\times\boldsymbol{Tx}(l_c/2)\times\boldsymbol{T}_{\mathrm{c}}\times & \\ \boldsymbol{Tx}(\Delta x-l_c/2) & l_c/2<\Delta x<l_c\\ \boldsymbol{T}_{\mathrm{A}}\times(\boldsymbol{T}_{\mathrm{cc}})^{m-1} & \Delta x=0\\ \boldsymbol{T}_{\mathrm{A}}\times(\boldsymbol{T}_{\mathrm{cc}})^{m-1}\times\boldsymbol{Tx}(l_c/2) & \Delta x=l_c/2\end{cases}\tag{26}$$

$$\boldsymbol{T}_{\mathrm{L}}=\begin{cases}\boldsymbol{Tx}(\Delta x_1-l_c/2)\times\boldsymbol{T}_{\mathrm{c}}\times\boldsymbol{Tx}(l_c/2)\times & \\ (\boldsymbol{T}_{\mathrm{cc}})^{n-2-m}\times\boldsymbol{T}_{\mathrm{A}} & l_c/2<\Delta x_1<l_c\\ \boldsymbol{Tx}(\Delta x_1)\times(\boldsymbol{T}_{\mathrm{cc}})^{n-2-m}\times\boldsymbol{T}_{\mathrm{A}} & 0<\Delta x_1<l_c/2\\ (\boldsymbol{T}_{\mathrm{cc}})^{n-m-1}\times\boldsymbol{T}_{\mathrm{A}} & \Delta x_1=l_c\\ \boldsymbol{Tx}(l_c/2)\times(\boldsymbol{T}_{\mathrm{cc}})^{n-2-m}\times\boldsymbol{T}_{\mathrm{A}} & \Delta x_1=l_c/2\end{cases}\tag{27}$$

5.1 Verification

Interference is most serious when the fault value is ∞. The rail voltage curves when fault value is ∞ are shown in Fig. 11.

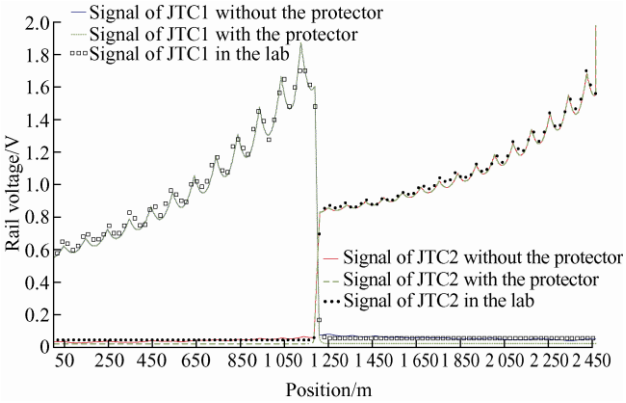

Fig. 11 Voltage curve of the track circuit without fault

According to Fig. 11, the over-zone signals have been suppressed with the protectors. The voltage value is lower, thus verifying the protector models.

5.2 Rail voltage of open-circuit BA1

The rail voltage curves of the track circuit with BA1 broken (Z_{gz1} is ∞) are shown in Fig. 12.

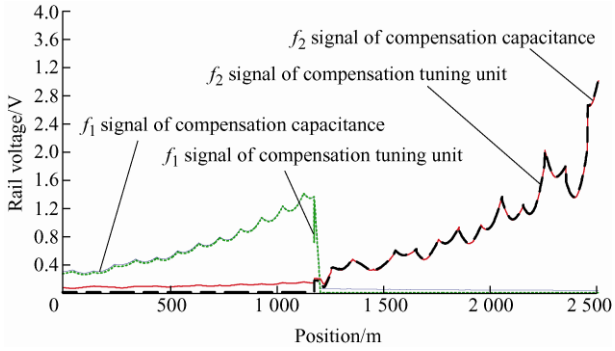

Fig. 12 Voltage curve of the track circuit with BA1 broken

As shown in Fig. 12, over-zone signals with the protectors can be greatly decreased across the protectors, and the protector is equivalent to a compensation capacitor for f_1.

5.3 Rail voltage with BA2 disconnection

The rail voltage curves of the track circuit with BA2 broken (Z_{gz2} is ∞) is shown in Fig. 13.

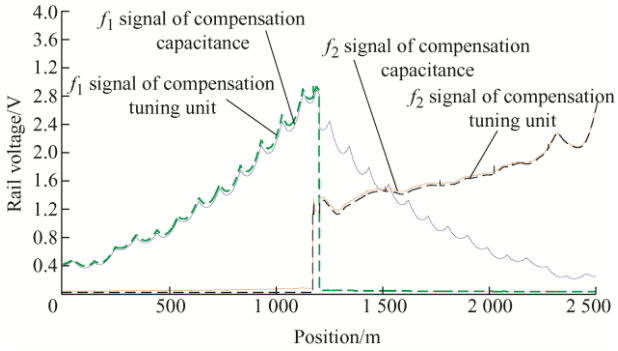

Fig. 13 Voltage curve of the track circuit with BA2 broken

Fig. 13 shows that the protectors protect the interference signal of f_1 in JTC2, and they do not bear on the resistance value of JTC2 with BA2 faults. The rail voltage of f_2 in JTC2 does not change and, after passing through protectors, the value of the f_2 signal of the track circuit with protectors was close to zero. This demonstrates that the protectors can improve protection ability against tuning area faults.

5.4 Rail voltage under a broken SVA condition

The rail voltage curves under the condition of SVA disconnection are shown in Fig. 14.

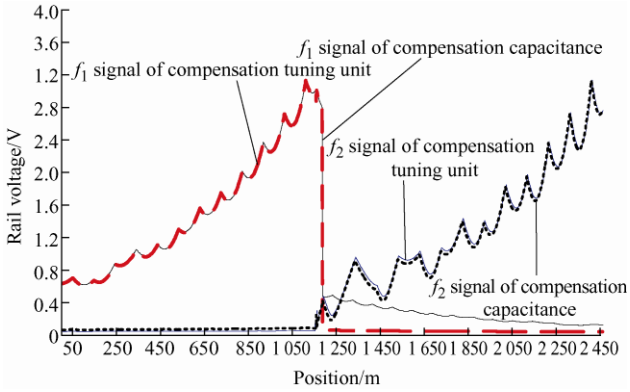

Fig. 14 Voltage curve of the track circuit with SVA broken

In Fig. 14, the extreme-impedance value of the two sections drops when SVA fails. Because the protectors can only improve the protection ability against zero-impedance faults, it cannot affect the signal of JTC1, but it can still decrease the value of the interference signal.

In Tabs. 2 and 3, it can be observed that f_1 signal in track section 1 with protectors is the same as that without protectors, and so is the f_2 signal in track section 2. However, the over-zone signals (f_2 signal in track section 1 and f_1 signal in track section 2) are close to 0. In other words, increasing the number of protectors can protect the over-zone signal and have the same effect on the transmission characteristics of the track circuit.

Tab. 3 Rail voltage of tuning area faults of JTC with protectors

State of track circuit	Value of faults	f_1 signal in track section 1	f_2 signal in track section 1	f_1 signal in track section 2	f_2 signal in track section 2
Normal	0	2.931 5	0.002 6	0.007 2	0.533 1
BA1 fault	0.1	2.772 2	0.002 9	0.008 4	0.482 7
	10	1.845 5	0.005 8	0.009 7	0.309 4
	∞	1.539 0	0.008 6	0.010 3	0.257 5
BA2 fault	0.1	2.877 8	0.002 8	0.010 5	0.497 5
	10	2.694 7	0.004 4	0.022 0	0.382 4
	∞	2.615 8	0.005 0	0.023 8	0.331 2
SVA fault	0.1	2.915 2	0.002 8	0.008 3	0.502 6
	10	2.865 3	0.003 2	0.008 9	0.436 9
	∞	2.794 2	0.003 5	0.009 4	0.404 3

5.5 Impact of protectors on safety

5.5.1 Equipment faults in the tuning area

Because monitoring staff will judge the faults in the tuning area according to the voltage of the receiver and shunting current, it is necessary to analyze the voltage of the track circuit with the protectors installed. Because the receiver has the function of frequency selection, the installation of protectors has no effect on the main track voltage of the receiver. The protective devices cannot affect the structure of the little track circuit and bear on the variation of the little track voltage at the receiving end. The protectors only change the zero-impedance value, which has no effect on the extreme-impedance value. Therefore, the staff can still judge the faults with the little track circuit voltage.

5.5.2 Compensation capacitor faults

The faults of the original compensation capacitor include disconnection, bad connection, short-circuiting and capacitor drops. Because compensation capacitors and protectors are connected with transmission cables, the influence on the transmission characteristics of the protectors is the same as those of the original compensation capacitors. According to the formulas of the calculated parameters, the protectors have the same effect on the transmission characteristics of the track circuit with compensation capacitors. The voltage curves of decreasing protectors is shown in Fig. 15.

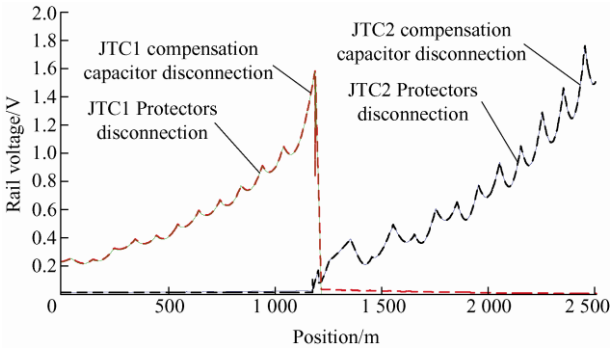

Fig. 15 Voltage of decreasing protectors

In Fig. 15, one can see that the rail voltage at the receiving end of JTC1 decreases when the protector is decreased, proving that decreasing protectors has the same effect on the transmission characteristics of the track circuit.

5.5.3 Broken rail situation

Because the integrity of the original track circuit can be checked in the whole process, it is necessary to analyze the checking ability of the track circuit with protectors. According to Fig. 2, the protector installed in the main track does not affect the electrical characteristics of the little track circuit, so it does not affect the broken rail inspection of the little track. If the point at which the rail is broken lies between the protectors and tuning area, the broken-rail fault

inspection can be completed according to the compensation capacitors to which the protectors are equivalent. If the broken track occurs between two protectors of the main track, then this is the same as the track circuit without protectors. In summary, the broken-rail fault inspection can be completed with the track circuit with protectors.

6 Conclusions

The effect of tuning area faults was studied according to the circuit resonance principle and transmission-line theory. Through a modeling analysis, the rail voltage in the normal state was found to vary. This can affect driving safety when the track circuit is occupied. In this study, according to the existing protection scheme, the method for calculating protector parameters has been provided and verified to be effective to protect against over-zone signals by simulation and experiments.

The simulation results demonstrate that the protectors can protect the adjacent section from interference when the zero-impedance equipment in the tuning area fails. Moreover, the transmission characteristics of the track circuit with the protectors are the same as those of the original one. Under a normal state of the track circuit, the protectors can effectively prevent over-zone signals with tuning area faults. Furthermore, the protectors have no impact on the normal operation and maintenance of the track circuit. Based on the frequency protection track circuit, the fault protection ability has been further improved.

The protection scheme has been applied to a new railway station in 2019 [20]. The protectors have been tested on a rail test line, and their reliability has been verified [21]. The installation of protectors is shown as Fig. 16.

Fig. 16 Installation of protectors on the rail

References

[1] Linhai Zhao, Lei Ren. Study on influence of JTC adjacent section interference on TCR. *Journal of the China Railway Society*, 2013, 35(12): 51-56.

[2] Zicheng Wang, Jin Guo, Yadong Zhang, et al. Fault diagnosis for jointless track circuit based on intrinsic mode function energy moment and optimized LS-SVM. *IEEE International Conference on High Voltage Engineering and Application*, Chengdu. IEEE, 2016: 1-4.

[3] Jiaxiang Xu, Wei Dong. ZPW-2000A jointless track circuit system modeling and simulation considering adjacent signal interference. *Proceedings of the 32nd Chinese Control Conference*, Xi'an. IEEE, 2013: 8780-8787.

[4] A Mariscotti, M Ruscelli, M Vanti. Modeling of audio frequency track circuits for validation, tuning, and conducted interference prediction. *IEEE Transaction on Intelligent Transportation Systems*, 2010, 11(1): 52-60.

[5] J Beak, Y Kim, Y Yoon. Analysis of return current effect for AF non-insulated track circuit in ITX vehicle operation. *Transactions of the Korean Institute of Electrical Engineers*, 2013, 62(4): 584-590.

[6] V Degardin, L Kone, F Valensi. Characterization of the high-frequency conducted electromagnetic noise generated by an arc tracking between DC wires. *IEEE Transactions on Electromagnetic Compatibility*, 2016, 58(4): 1228-1235.

[7] J Chen, C Roberts, P Weston. Fault detection and diagnosis for railway track circuits using neuro-fuzzy systems. *Control Engineering Practice*, 2008, 16(5): 585-596.

[8] Zhiyang Yu, Kuifang Yang, Fengming Shen. Study on transmission performance of ballastless track circuits. *Journal of the China Railway Society*, 2007, 29(5): 122-126.

[9] S Won, J Choi, H Park. An analysis of voltage characteristics for LC resonant frequency band of capacitor compensation according to moving of electrical separation equipment of AF track circuit. *Transactions of the Korean Institute of Electrical Engineers*, 2016, 65(8): 1466-1477.

[10] T Nomura, H Arai, H Fujita. A study of failure factor of resonant capacitor for impedance bond. *International Conference on Lightning Protection*, 2018: 157-162.

[11] Xiaochun Wu, Guanggang Ji. Research on a kind of protection choke matching transformer for track circuit. *Journal of Applied Science and Engineering*, 2018, 21(1): 69-76.

[12] Xiaochun Wu, Guoqing Li. Research on immunity to electric impulsive interference of ZPW-2000 track circuit in station. *International Journal of Security and Its Applications*, 2016, 10(1): 257-264.

[13] Qizhi Ma, Xuqin Xie, Zhuohui Deng, et al. Research on railway harmonic suppression based on high-pass filter. *Journal of Electrical Engineering*, 2017, 12(2): 1-7.

[14] Yunjie Shi, Xiayun Feng, Fei Wang, et al. Instability mechanism and control measures of reactive compensation in islanded microgrid based on droop control. *Journal of Electrical Engineering*, 2020, 15(1): 29-35.

[15] Yipeng Song, Heng Nian, F Blaabjerg. Resonance active damping and PCC voltage quality improvement of DFIG system connected to parallel compensated grid. *Chinese Journal of Electrical Engineering*, 2018, 4(4): 33-40.

[16] V T Hung, Hongchun Shu, L N Giang. Double-loop control structure using proportional resonant and sequence-decoupled resonant controllers in static coordinates for dynamic voltage restorer. *Chinese Journal of Electrical Engineering*, 2019, 5(3): 10-19.

[17] Ministry of Railways of the People's Republic of China. Railway signal maintenance rules. Beijing: China Railway Publishing House, 2007.

[18] National Railway Administration of the People's Republic of China. Technical specification of ZPW-2000 track circuit: TB/T 3206——2017. Beijing: China Railway Publishing House, 2017.

[19] Beijing National Railway Research & Design Institute of Signal & Communication. Frequency protection tuning non-insulated track circuit. China, 02235257.0. 2005-07-20.

[20] Wentao Li. Research on protection measures on interference of damaged insulation in track circuit of railway station. *Railway Signalling & Communication*, 2018, 54(5): 23-26.

[21] Xian Zhang. Research on encapsulation technology of compensation tuning unit for track circuit. *Railway Signalling & Communication Engineering*, 2019, 16(S1): 23-26.

Yunshui Zheng was born in Gansu Province, China, on July 22, 1972. He graduated in electrical engineering and automation from Lanzhou Jiaotong University, Gansu, China, in 1994. He is a professor at Lanzhou Jiaotong University, Lanzhou, China.

In recent years, he has published more than 20 papers in domestic journals and important conferences, and participated in the completion of six NSFC projects. At present, he is mainly engaged in teaching and scientific research related to railway automatic control, railway system reliability, and railway building information modeling (BIM) technology.

Zhanyi Shu was born in Heilongjiang Province, China, on November 18, 1991. He is a master candidate in traffic information engineering and control at Lanzhou Jiaotong University, Lanzhou, China.

His main research interests concern reliability and safety of jointless track circuits.

Shenglin Gao was born in Gansu Province, China, on June 11, 1989. He got a master degree in traffic information engineering and control at Lanzhou Jiaotong University, Lanzhou, China.

His main research interests are traffic communication and centralized traffic control (CTC).